TOMOGRAPHIC RECONSTRUCTION OF A BEAM PHASE SPACE FROM LIMITED PROJECTION DATA*

G. Asova†, S. Khodyachykh‡, M. Krasilnikov, F. Stephan, DESY, 15738 Zeuthen, Germany
I. Tsakov, INRNE BAS, Sofia, Bulgaria

Abstract

The production of electron beams suitable for the successful operation of the European XFEL is studied at the Photo-Injector Test Facility at DESY, Zeuthen site (PITZ). The PITZ beamline is equipped with three dedicated stations for transverse emittance measurements and in the forthcoming shutdown period a section for transverse phase-space tomography diagnostics will be installed. The module contains four observation screens and therefore only four projections can be used in order to reconstruct an underlying phase-space density distribution.

This work presents the performance of a number of reconstruction algorithms on limited projection sets using numerical data applied to the PITZ operating conditions. Different concepts for comparison between an original phantom and the reconstructed distribution are presented.

INTRODUCTION

The PITZ facility is dedicated to the development and optimization of electron sources subsequently to be used in FELs like the FLASH and the future European XFEL. Such goals require detailed knowledge of the electron beam properties according to which the PITZ beamline is equipped with extensive diagnostics components. A key element for the performance of a FEL is the small transverse emittance, wherefrom the transverse phase space is a central point in the electron source characterization at PITZ. Currently, the transverse phase space is being reconstructed using single slit scan technique [1] and a new module for transverse phase space tomography diagnostics will be installed in the forthcoming 2009-upgrade.

The module consists of four screen stations as each two surround a FODO cell. Correspondingly, four projections are to be used for tomographic reconstruction. The design has been discussed in [2] and expectations towards its performance with nominal beam parameters of 1 nC bunch charge, 32 MeV/c momentum and normalized transverse emittance of 1 mm mrad can be found in [3]. The setup will also be used in a combination with a transverse deflecting cavity structure to study the longitudinal phase space of individual pulses within the bunch train. In any case the choice of proper reconstruction algorithm is of great importance.

* This work has partially been supported by the European Community, contract No. RII3-CT-2004-506008 and 011935.

† galina.asova@desy.de

‡ Presently at Siemens AG, Rudolstadt, Germany.

This work focuses on the performance of a few reconstruction algorithms with respect to their applicability to limited input projection data. The methods discussed are Filtered Backprojection (FBP), Constrainted Additive Algebraic Reconstruction Technique (caART) and Maximum Entropy (MENT). Several approaches to quantify the quality of the reconstruction conclude the contribution.

TRANSVERSE PHASE-SPACE TOMOGRAPHY OF AN ELECTRON BEAM

Tomography deals with the reconstruction of an n-dimensional object knowing an infinite number of its $(\mathrm{n}-1)$-dimensional projections calculated at different view angles in $[0,\pi]$. A great number of scientific and practical areas are using the tomography ideas - medical imaging is interested in innocuous cross sectioning of the human body, archaeology needs non-destructive material inspection.

The object of interest in the transverse beam dynamics is an underlying density distribution $\rho\left(x,x',y,y'\right)$ at a given position along the beamline. The density distribution cannot be obtained instantly but its spatial components are directly measurable by means of screens, wire scanners, etc. Meeting an observation screen, for instance, the four-dimensional phase space is projected onto a spatial distribution (x,y). A number of projections of the spatial distribution, taken at different angles, are needed for the reconstruction and, therefore, one needs to vary the orientation of the phase space on the screen. The last is equivalent to rotation of the beam in the phase space and is achievable by altering the focusing conditions using magnets. Let the system be linear such that M denotes a valid 2×2 transformation matrix from the position of reconstruction z_i to the position of observation z_f and $p\left(x_f\right)$ is a projection onto the horizontal axis at z_f. The condition on the linearity should be interpreted so that the matrices M describe well the transport between the two longitudinal positions. The projection can be written as a function of the initial phase-space coordinates as the Radon transform

$$p(x_f)=\iint \rho\left(x_i,x_i'\right)\delta\left(x_f-M_{11}x_i-M_{12}x_i'\right)dx_i dx_i'. \tag{1}$$

The problem to be solved is, having a number of $p\left(x_f\right)$ with different matrices M, to find a unique inversion of the Radon transform. Disregarding any intrinsic measurement errors, the singularity of the solution depends on the number of projections, the equidistant steps between each

two of them and the linearity of the system. While the latter might be hard to cope with and the first two strongly depend on the hardware setup, the overall result can be optimized applying a suitable reconstruction algorithm.

RECONSTRUCTION ALGORITHMS

Backprojection (BP) and its derivative Filtered Backprojection (FBP) [4] attain fast computations and are simple to implement making them two of the most commonly used reconstruction methods. BP employs direct inversion of the Radon transform (1) as it iteratively smears each projection onto the position of reconstruction according to the fact that the density at a point can be defined as integration over the line integrals from different projections passing through this point or

$$\rho\left(x, x'\right) = \int_0^{\pi} p_\theta\left(x_\theta\right) d\theta \tag{2}$$

for θ determining the transformation. Defined in this way, the inversion of the Radon transform is influenced by blurring effects due to the fact that each point might be added more than once since it might contribute not to a single line integral in the space (x, y). The FBP uses an additional low pass filter which introduces negative values in each projection. The latter ones are needed in order to correct for projections from other angles. The filter is applied in advance to the iterative smearing.

When applied to limited data sets the performance of BP and FBP is unsatisfactory. This is shown in Fig. 1, where

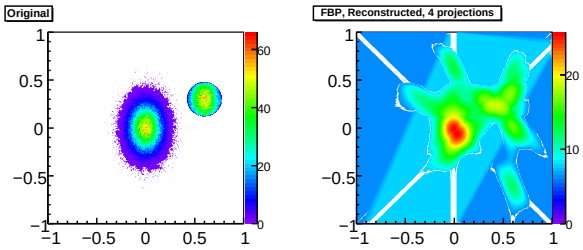

(a) Original distribution. (b) Result using 4 projections.

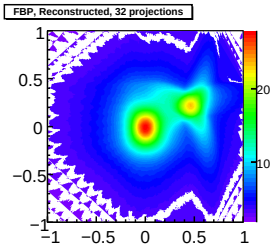

(c) Result using 32 projections.

Figure 1: Comparison between original distribution and its reconstructed ones using FBP with different number of input projections. The ridges on the reconstructed distribution decrease with the number of angular steps.

an original phantom distribution is given beside the reconstruction result of FBP having four projections, obtained with equidistant rotations over π - Fig. 1(b). Fig. 1(c) shows that the quality of the reconstruction in terms of streaking artifacts improves with the increase of the number of projections. For that particular example each projection is convoluted with a Butterworth low-pass filter [4] priori the integration. Filtering out low intensity values would not be sufficient since the uniform spot on the right hand side of Fig. 1(a) is still not well defined even in the case of 32 projections.

FBP is not a recursive algorithm - the process of reconstruction depends on one projection at an iteration step and can consequently be completed disregarding any supplementary input. The availability in advance of all projections to be used is required for recursive algorithms like ART [5], as MENT [6] is regarded here as a derivative of the algebraic techniques solving a minimization task in a different manner.

The ART, as the name implies, uses a matrix-like indirect approach to the inversion problem - the different projections are considered as a set of linear equations with the values of the function to be reconstructed as unknown variables. If the wanted density distribution is described as constituted of K pixels and w_{nk} represents the contribution of the k-th pixel to the n-th projection, with n denoting some of the available N projections, a projection can be written in the form

$$p_n = \sum_{k=1}^{K} w_{nk}\rho_k. \tag{3}$$

Solution of a system of linear equations like Eq. (3) is to be found.

ART is an iterative algorithm - the wanted density of a bin is calculated over a number of steps as on each step projections of the current guess are snapped. The repetitive procedure continues until the computed projections resemble the given ones according to some set of criteria. Additive ART (aART) applies a correction to the k-th pixel on the $(i+1)$ iteration step of the kind

$$\Delta\rho_k^{(i+1)} = \left(\frac{p^{(i+1)} - q^{(i+1)}}{\sum_{j=1}^{K} w_{(i+1)j}^2} \right) w_{(i+1)k}, \tag{4}$$

where $q^{(i+1)}$ is the projection calculated from an iterative guess $(i+1)$ and $p^{(i+1)}$ is the one, given in advance from the measured data.

If the system described by the equations like (3) is underdetermined, i.e. the number of pixels is more than the number of projections, a unique solution does not exist. Such is the case for the PITZ setup of four screens and also for reconstruction applied on double-quadrupole scan data. On the other hand, there might be none or multiple solutions for an overdetermined system. The MENT algorithm gives

a possibility to select an outcome most consistent with the measured data. As it is used here MENT has already been described in [6, 3].

Fig. 2 shows the results of aART and MENT applied to the same four projection as in Fig. 1(b). An additional constraint for non-negative pixel content has been applied to the ART, usually known as Constrainted Additive ART (caART), and MENT requires such by definition. The quality of the resulting distributions is visibly improved as expected according to the fact that a minimization task would be needed for an underdetermined system. Smearing artifacts like those that can be seen in the outcome of FBP are not present, the projected area of the central gaussian distribution is refined as well as is the uniform spot on the right hand side.

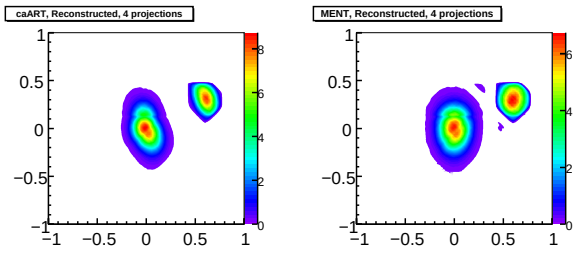

(a) caART result. (b) MENT result.

Figure 2: caART and MENT applied to four equidistant rotations. The object of reconstruction is the one in Fig. 1(a).

RECONSTRUCTION FROM NUMERICAL DATA

The decision for choosing a suitable reconstruction algorithm depends on its performance on numerical data. Here the caART and MENT are applied on a simulated electron beam distribution, matched to the optics of the lattice and tracked with ASTRA [8]. The influence of space-charge forces is included in the tracking as they tend to be significant for the PITZ operating conditions. The periodicity of the particle trajectories is expressed with the mismatch of the measured Twiss β-functions from the design values at the positions of observation. The numerical tracking reveals maximum β-mismatches of 3 and 6% for the horizontal and the vertical planes respectively. Fig. 3 shows the original phase-space and the resulting reconstructions for the horizontal plane. Both methods manage to reproduce the double-like structure in the core of the beam as visually MENT surpasses in better restoration of the density in the tails. Table 1 contains the relative deviations of the reconstructed distributions with respect to the original.

As an alternative measure of the quality of the reconstruction, constructive for distributions non-symmetric in neither of the x or x' planes, the skewness could be used.

Except with the second central moments and the covariance, needed in order to determine the transverse emittance, the quality of the reconstruction should be judged from point of view of what charge density it represents. A convenient interpretation is offered by the mean square norm

$$\|\Delta\| = \sqrt{\frac{\sum_x \sum_{x'} \left(\rho_{orig} - \rho_{recon}\right)^2}{\sum_x \sum_{x'} \rho_{orig}^2}}, \qquad (5)$$

where ρ_{recon} and ρ_{orig} denote the resulting reconstruction and the original distribution correspondingly. For such an estimation to be valid, effects from low-density bins should be discarded and the bin size of the two objects has to be equal. ASTRA calculates the moments of the distribution in a statistical manner, whereas here two discrete binned distributions are compared. If the binning does not represent the underlying data according to its specific features, lateral bins with low content would introduce gaussian tails and consequently differently calculated beam sigma matrix elements. This has been taken into account in advance as the bin width δ has been optimized using a minimization of a cost function $F(\delta)$ according to

$$F(\delta) = \frac{2\mu - var}{\delta^2} \qquad (6)$$

for μ and var being the mean and the variance of the underlying spatial distribution [7] . Using the norm and the

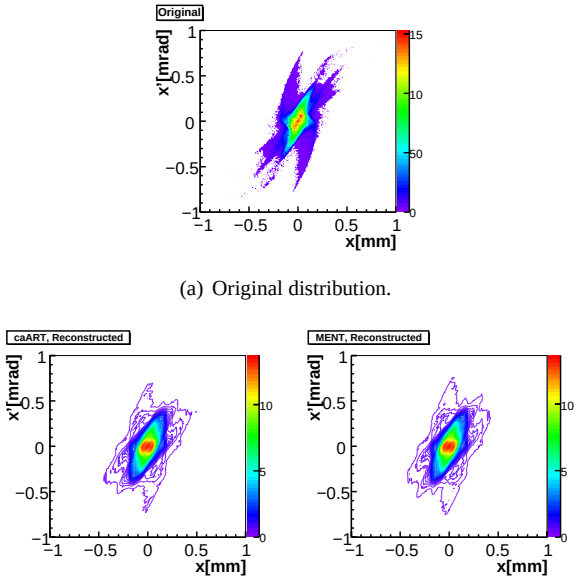

(a) Original distribution.

(b) caART result. (c) MENT result.

Figure 3: Realistic distribution and its reconstructed using caART and MENT.

Table 1: Relative errors between the original distribution and its reconstructed from Fig. 3.

Algorithm	σ_x [%]	$\sigma_{x'}$ [%]	$\sigma_{xx'}$ [%]
caART	1.59	3.57	5.94
MENT	0.75	0.64	2.33

reconstructions above, MENT and caART yield equal values until the second digit after the decimal point. In the first case the norm is $\|\Delta\| = 0.247$ and at the second $\|\Delta\| = 0.258$.

An alternative for the comparison is based on the equivalent ellipse emittance representation of the phase space, i.e. compare the resulting and original distributions from which only parts within ξ times the projected emittance are taken into account. Low intensity bins outside the contour defined by $\xi.\varepsilon$ are discarded. The projected emittance is calculated separately for each of the two distributions - the original ASTRA one, describing the real phase space in some of the transverse planes, and the reconstruction. By this, the total area in the phase space is defined and a two-dimensional 'peel-off' cut on the tails is applied afterwards. The resulting fractional areas inside the contour are considered in order to calculate the norm. The outcome in such a case slightly favors the MENT - $\|\Delta\| = 0.249$, while for the ART this value is 0.260. This can also be seen in Fig. 4 where different fractions of the distributions are taken into account. The horizontal lines represent the case when the two distributions are compared within their total area. For fractional area of above six the norm converges to the value for which no cut has been done as MENT solutions are closer. i.e. the core part is always reconstructed smoother with better accuracy than using ART.

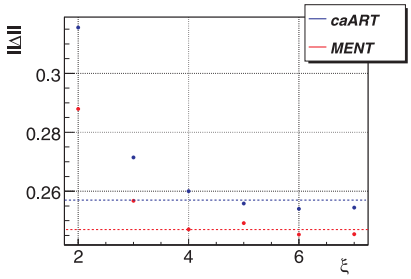

Figure 4: Mean square norm for different cuts of the phase-space distributions. A cut is done simultaneously on the original and the reconstructed phase spaces. The transverse emittances defining the area of the cut are calculated separately from the data describing the original and the reconstructed distributions. The horizontal lines indicate that the full phase spaces have been taken into account.

CONCLUSIONS

The work presents some investigations done in order to find a tomographic reconstruction algorithm suitable to be used with limited projection data. Several algorithms have been tested, namely Filtered Backprojection, Constrainted Additive Algebraic Reconstruction Technique and Maximum Entropy. The last two inherit the ideas behind the FBP and as such they outperform it - a major reason for that is the fact that both are trying constructively to discard pixel content which are not consistent for any of the projection data. A number of concepts on how the reconstruction results have been evaluated are presented as well. A conclusion that MENT represents the underlying phase space with better accuracy can be drawn.

REFERENCES

[1] L. Staykov, "Characterization of the transverse phase space at the Photo-Injector Test Facility in DESY, Zeuthen site", PhD thesis, Universität Hamburg, 2008.

[2] G. Asova et al., "Design considerations for phase space tomography diagnostics at the PITZ facility", proceedings of DIPAC 2007, Mestre, Italy.

[3] G. Asova et al., "Phase space tomography diagnostics at the PITZ facility", proceedings of ICAP 2006, Chamonix, France.

[4] R. M. Rangayyan, "Biomedical Image Analysis", CRC Press, 2005.

[5] R. Gordon, "A tutorial on ART (Algebraic Reconstruction Technique) ", *IEEE Trans. Nucl. Sci.*, NS-21(78), 1974.

[6] G. Minerbo, "A Maximum Entropy Algorithm for Reconstructing a Source from Projected Data", Comp. Graphics Image Proc. 10 (1970) 48.

[7] H. Shimazaki, "Recipes for Selecting the Bin Size of a Histogram", PhD thesis, Kyoto University, 2007.

[8] K. Flöttmann. http://www.desy.de/˜mpyflo/.